SLAC-PUB-2529
June 1980
(T/E)

MASTER

CHARMONIUM STUDIES WITH THE CRYSTAL BALL*

CONF-800374--9

M. Oreglia
(Representing the Crystal Ball Collaboration[1])
Stanford Linear Accelerator Center
Stanford University, Stanford, California 94305

Abstract: The Crystal Ball detector at SPEAR is used to analyze the decays $\psi' \to \gamma\gamma\psi$ and $\psi' \to \gamma\chi, \chi \to \gamma\gamma$. Values are obtained for the branching ratios of $\psi' \to \eta/\pi^0\psi$ and $\psi' \to \gamma\chi, \chi \to \gamma\psi$. No evidence is found for a $2^1S_0(\eta_c')$ state in the mass range 3129 → 3644 MeV/c^2. Analysis of the angular distributions in the cascade χ decays yields spin and multipole assignments for the $\chi(3.51)$ and $\chi(3.55)$.

Résumé: On utilise le détecteur "Crystal Ball" à SPEAR pour analyser les désintégrations $\psi' \to \gamma\gamma\psi$ et $\psi' \to \gamma\chi, \chi \to \gamma\gamma$. On a obtenu des valeurs pour les rapports de branchement de $\psi' \to \eta/\pi^0\psi$ et $\psi' \to \gamma\chi, \chi \to \gamma\psi$. On n'a pas trouvé d'état $2^1S_0(\eta_c')$ dans le domaine de masse 3129 → 3644 MeV/c^2. L'analyse des distributions angulaires dans les désintégrations des cascades des χ permet de déterminer le spin et les coefficients multipolaires de $\chi(3.51)$ et $\chi(3.55)$.

(Presented at the XVth Rencontre de Moriond: Electroweak and Unified Theory Prediction, Les Arcs, France, March 15-21, 1980.)

* Work supported by the Department of Energy under contract DE-AC03-76SF00515.

I. INTRODUCTION

The decays

$$\psi' \to \gamma\gamma\psi, \quad \psi \to e^+e^- \text{ or } \mu^+\mu^- \tag{1}$$

reveal some of the most fundamental properties of the charmonium system; indeed, measurement of the states between the ψ and ψ' provides a basic test of the charmonium model. I shall report on a comprehensive study of the cascade decays

$$\psi' \to \gamma'\chi, \chi \to \gamma\psi \tag{2}$$

as well as

$$\psi' \to m\psi \tag{3}$$

where m denotes a mass state such as η or π^0, and γ' denotes the monochromatic photon. Data for this study was obtained using the Crystal Ball detector at SPEAR, from November 1978 to May 1979. Approximately 6 weeks of data acquisition in 4 intervals provided ~1600 nb^{-1} of data, from which 776k ± 78k $\psi'(3684)$ are used for this analysis. The error on the number of ψ' arises from subtraction of beam gas, cosmic ray and continuum events.

Concentrating on the states between the primary and first radially excited $^3S_1$ states of the charmonium model, one expects transitions to four intermediate χ states, namely three $1^3P_{0,1,2}$ levels and the pseudoscalar 2^1S_0 (the η_c'). So far, the experimental picture has remained somewhat controversial. Inclusive γ spectra from the ψ' reveal three states with masses 3.41, 3.51 and 3.55 MeV/c^2, but no hint of a fourth intermediate state. Assuming that a state observed with mass 2.98 GeV/c^2 is the $1^1S_0(\eta_c)$,[2] the 2^1S_0 state should lie about 70 MeV below the ψ', consequently the factor E_γ^3 suppresses the rate for $\psi' \to \gamma'\eta_c'$.[3] Furthermore, the η_c' might be a broad state ($\Gamma \simeq 20$ MeV), as may be indicated for the η_c candidate. For these reasons, the η_c' is difficult to observe in inclusive spectra. A study of the cascade exclusive channel also clearly shows the $\chi(3.51)$ and $\chi(3.55)$, however there has been uncertainty about $\chi(3.41)$ in this channel. In addition, states with masses of 3.45[4] and 3.59[5] (or 3.18) MeV/c^2 have been reported.

Spin information on the intermediate states can be obtained from their hadronic decay modes. Since the ψ and ψ' are well established $J^{PC} = 1^{--}$ states, the χ states can have the assignments $J^{PC} = (0,1,2)^{P+}$ which accomodate a radiative transition. The $\chi(3.41)$ is observed to decay into two pseudoscalars ($\pi\pi$ and $K\bar{K}$),[6] thus is 0^{++} or 2^{++} (C-parity forbids 1^{--}). Additional evidence from the inclusive spectrum for a $1+\cos^2\theta$ distribution of γ' (relative to the e^+e^- beam)[6] supports a 0^{++} assignment. Assignments for the other two χ levels have not been as certain. The $\chi(3.55)$ is also observed to decay into two pseudoscalars, and deviates from a $1+\cos^2\theta$ distribution by 1.6 standard deviations,[6]

hence is indicated to be 2^{++}. Observation of $\chi(3.51) \to \pi KK_S$[7] prohibits 0^+, while the γ' angular distribution appears to discriminate against spin-0 altogether; this leaves the unnatural spin-parity assignments of 1^{++} and 2^{-+} as possibilities.

An alternate method of obtaining the spin of intermediate states is to study the γ'-γ correlations for the cascade sequence. This method, long practiced by nuclear physicists,[8] was first applied to cascade data by Tanenbaum,[6] but did not provide unique assignments due to a small data sample. We have successfully employed this technique on a large sample of 921 $\chi(3.51)$ and 441 $\chi(3.55)$ events to obtain both spin and multipole information for the individual radiative transitions.

II. APPARATUS

Investigation of the radiative transitions of charmonium requires detection of photons in the 0-600 MeV range, for which the Crystal Ball detector is well suited. The principle components of the apparatus are shown in Fig. 1. Immediately surrounding the interaction region are three chambers for charge identification and tracking. Innermost and outermost are the magnetostrictive spark chambers, covering 94% and 71% of 4π sr, respectively; sandwiched between these is a multi-wire proportional chamber which covers 86% of 4π sr. Charge identification therefore exists over 94% of 4π sr, however complete tracking requires the use of both spark chambers, thus is limited to 71% of 4π sr. The spark chambers are capable of reconstructing charged trajectories for 86% of the leptons from (1), with a resolution $\sigma = 0.3^\circ$. Overall efficiency of the chambers for identification of both leptons in reaction (1) is 96%, although conversion of photons from (1) before leaving the chambers adds an additional efficiency factor of 95%.

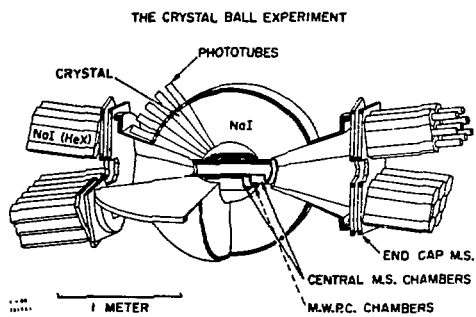

Fig. 1. Schematic diagram of the Crystal Ball detector.

Surrounding the chambers is the Crystal Ball proper (the detector uses no magnetic field). This consists of 672 NaI(Tl) crystals, each 16 radiation

lengths (= 16 inches) long, and stacked in the manner of a geodesic dome covering 94% of 4π sr. The crystals are hermetically sealed in two hemispheres which are normally in contact, although they may be separated by up to 1.5 meters to permit access to the chambers. Augmenting the Ball proper are endcap quadrants consisting of planar magnetostrictive spark chambers followed by 20 inch long hexagonal NaI(Tℓ) crystals. A total of 60 crystals comprises these endcaps, bringing the total solid angle covered by NaI(Tℓ) to 98% of 4π sr. More details on the apparatus can be found elsewhere.[9]

III. ANALYSIS OF DATA

Energy of electromagnetically showering particles (i.e., γ and $e^{\pm}$) is measured in the NaI(Tℓ) with a resolution $\sigma = 0.028 \times E^{.75}$ GeV. Clusters of 13 contiguous crystals (each about 2% of the Ball) measure 98% of the shower energy. Analysis of the energy pattern in these clusters permits tracking of photons, as well as $e^{\pm}$ not tracked in the chambers, with a resolution $\sigma = 1.5^{\circ}$–2° (higher energy photons having the superior resolution). A muon from (1) deposits minimum ionizing energy (with a peak at 210 MeV) in the NaI(Tℓ), and there is a small amount of multiple scattering. The pattern technique permits NaI(Tℓ) tracking of muons with $\sigma = 3.2^{\circ}$.

To insure a trigger efficiency better than 99% for (1), we restrict the analysis to events having all four particles within the central 90% of 4π sr relative to the e^+e^- beams (i.e., $|\cos\theta| < 0.9$). In addition, events are rejected if the measured angle between any two tracks is less than 26° (the angle subtended by two crystals). A software threshold of 20 MeV is applied to all tracks, and those with $20 < E_{track} < 40$ MeV and within 32° of an energetic ($E_{track} > 900$ MeV) $e^{\pm}$ are considered to be fluctuations in the electron's shower pattern, hence are absorbed into the $e^{\pm}$ track. An event is considered as an initial candidate for (1) if only 2 leptons and 2 photons are observed in the allowed solid angle, and the endcaps display a total energy less than 8 MeV. The endcap cut effectively suppresses the $\pi^0\pi^0$ background described below. Calculated neutral energy for (1) lies in the range 542–589 MeV, permitting the additional requirement that candidates for (1) have measured neutral energy in excess of 490 MeV. Finally, an exceedingly clean sample is obtained by requiring that each photon energy exceed 40 MeV. The remaining events are fitted kinematically to the hypothesis that they arise from reaction (1); this fit is 5C(3C) for $e^+e^-(\mu^+\mu^-)$ final states. Confidence level distributions are flat when we require C.L. > 0.005. The overall acceptance for (1) after all cuts and efficiencies have been taken into account is 0.4–0.5, except for the π^0 events, which have an efficiency of about 0.3.

The 2225 events surviving all of the above cuts are shown in the scatterplot of Fig. 2b; various features are demonstrated in Fig. 2a. By $(M_{\psi\gamma})_{high}$ we refer to the mass formed from the ψ and the higher energy photon. Evident in Fig. 2b are $\chi(3.51)$, $\chi(3.55)$, η and indications of $\chi(3.41)$ and π^0. The principal background for (1) comes from $\psi' \to \pi^0\pi^0\psi$ when 2 of the 4 photons from the pions escape detection. Our large NaI(Tℓ) solid angle and the energy cuts limit this background to 7 events. This prediction follows from a Monte Carlo study using the measured $\pi\pi$ mass distribution.[7] Before the kinematic fitting and C.L. cut, 140 background events are expected, none having $\gamma\gamma$ masses less than 200 MeV/c^2. Eight events in Fig. 2b are found to be hadron events, which are easily identified by the hadronic energy deposition pattern in NaI(Tℓ) when the events are hand scanned; these events are removed from subsequent plots.

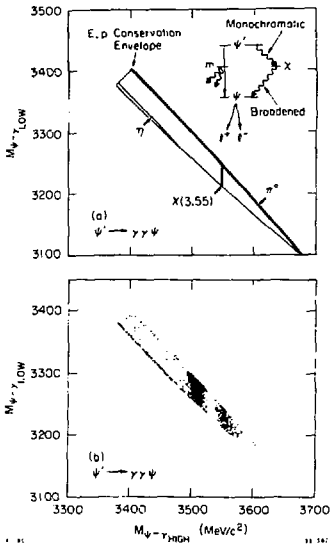

Fig. 2. The scatterplot of high and low γ-ψ masses for $\psi' \to \gamma\gamma\psi$ candidates. (a) depicts the kinematic boundaries for the process, and the appearance of some features. (b) shows the data fitted kinematically to reaction (1).

IV. $\psi' \to \eta/\pi^0\psi$

The $\gamma\gamma$ mass distribution for events in Fig. 2b is shown in Fig. 3a, along with the Monte Carlo prediction for $\pi^0\pi^0$ background. A peak from η at 547.3 ± 1.4 MeV/c^2 has the expected width ($\sigma = 1.2\%$) for an η produced in reaction (3). We separate η from χ events by cutting at $m_{\gamma\gamma} > 525$ MeV/c^2; this cut loses no η, however our Monte Carlo predicts that it admits 21 $\chi(3.51)$ and 5 $\pi^0\pi^0$ background events to the η sample. After subtraction we observe 386 η; correcting for efficiency and the $\eta \to \gamma\gamma$ branching ratio of 0.38, we obtain

$$BR(\psi' \to \eta\psi) = (2.18 \pm 0.14 \pm 0.35)\% \quad .$$

The first error covers statistics and uncertainty in the efficiencies, while the

second error is systematic, arising from uncertainty in the number of ψ' produced and in $BR(\psi\psi \to e^+e^-)$.[10] Our value for the η branching ratio agrees well with the value $(2.5 \pm 0.6)\%$ obtained recently by the Mark II group,[11] however both the new SPEAR values are smaller than previous measurements of 3.5 ± 0.7,[12] 3.6 ± 0.5[5] and 4.3 ± 0.8[13] by almost a factor of 2. We might attribute this change to a better understanding of the background from $\pi^o\pi^o$.

Evidence for the π^o from (3) is obscured in Fig. 3a by the χ events. These are removed by rejecting events with $(M_{\psi-\gamma})_{high}$ in the ranges 3410 ± 5, 3470-3590 MeV/c^2 and with $m_{\gamma\gamma} > 525$ MeV/c^2 to obtain Fig. 3b. A clear π^o signal is seen at a mass of 136.1 ± 2.5 MeV/c^2, having a width ($\sigma = 7.7\%$) consistent with that of a π^o from (3). A Gaussian plus quadratic fit yields 23 π^o events above background, and 8 background events with $m_{\gamma\gamma} < 200$ MeV/c^2. This background fit is consistent with our Monte Carlo prediction of 15 background events with $m_{\gamma\gamma} < 200$ MeV/c^2. The resulting value for the branching ratio is

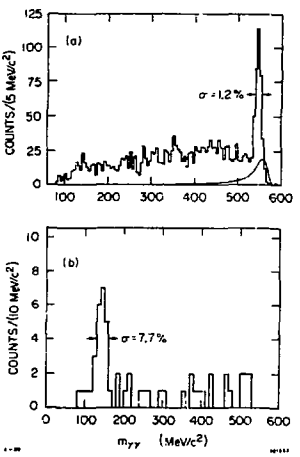

Fig. 3. $\gamma\gamma$ mass distributions. (a) shows the distribution for all events $\psi' \to \gamma\gamma\psi$; the curve shows the Monte Carlo distribution for $\pi^o\pi^o$ background (magnified × 30). Events with $(M_{\psi-\gamma})_{high}$ in the regions 3410 ± 5 and 3530 ± 60 MeV/c^2 and with $m_{\gamma\gamma} > 525$ MeV/c^2 have been removed in (b).

$$BR(\psi' \to \pi^o\psi) = (0.09 \pm 0.02 \pm 0.01)\%$$

where the errors are quoted as in the η measurement. The π^o events could conceivably arise from non-resonant production (i.e., $e^+e^- \to \pi^o\psi$), so we have checked this by examining 1772 nb^{-1} of data at $E_{CM} = 3772$ MeV. From this analysis we find that continuum $\pi^o\psi$ production at $E_{CM} = 3684$ MeV has a 90% C.L. upper limit branching ratio of 0.01%. Our result for $BR(\psi' \to \pi^o\psi)$ agrees with a measurement by the Mark II group[11] of $(0.15 \pm 0.06)\%$ based on observation of 7 events with a background of 1.1. Observation of the π^o decay with a branching ratio of order 10^{-3} suggests that isospin symmetry is broken.[14] The decay (3) is not allowed for π^o, since ψ' and ψ have isospin 0. Although the decay may occur electromagnetically, one expects a rate about 17 times smaller than that observed. The additional rate is expected to arise from an amplitude which directly breaks

isospin symmetry, as in the decay $\eta \to 3\pi$.

V. THE χ STATES

Cascade events are separated from the data by subtracting η and π^0 events using the criteria $m_{\gamma\gamma} < 525$ MeV/c^2 and $|m_{\gamma\gamma} - 135| > 25$ MeV/c^2; this sample is shown in Fig. 4a, and the projection on the $(M_{\psi-\gamma})_{high}$ axis is shown in Fig. 4b. The $E_{track} > 40$ MeV cut excludes χ states with $(M_{\psi-\gamma})_{high} > 3644$ MeV/c^2, as indicated in Fig. 4a, and with $(M_{\psi-\gamma})_{low} < 3129$ MeV/c^2. The 6 events denoted by enlarged dots all have e^+e^- as final state. Closer inspection of the individual event displays reveals that $(M_{\psi-\gamma})_{high}$ was measured too low in these cases, because of overlap of the low energy photon with the energetic electron's shower. It therefore appears that these 6 events constitute a tail from the $\chi(3.51)$; this is also evident from the projection in Fig. 4b. Aside from the 6 special events, we observe very little activity in the regions $(M_{\psi-\gamma})_{high} = 3.45$ and 3.59 GeV/c^2 -- we observe no hint of a fourth χ states. Strong evidence for the cascade of $\chi(3.41)$ is apparent in Fig. 4a, where 2-3 of the 20 events in the 3.41 GeV/c^2 region are expected to be background from $\pi^0\pi^0$. For all decays measured in this analysis, observed e^+e^- and $\mu^+\mu^-$ final states are equal in number to within 10%, thus consistent withia statistics. The branching ratios resulting from observation of 17 $\chi(3.41)$, 943 $\chi(3.51)$ and 479 $\chi(3.55)$ events are listed in Table I, along with 90% C.L. upper limit branching ratios for χ with masses 3.45 and 3.59 GeV/c^2 (assuming the quantum numbers $J^{PC} = 0^{-+}$). In the $\chi(3.45)$ case, upper limits obtained by using both the full data (including the 6 special e^+e^- events) and by using only the $\mu^+\mu^-$ final states are given. The errors shown in Table I are quoted in the same manner as the previous branching

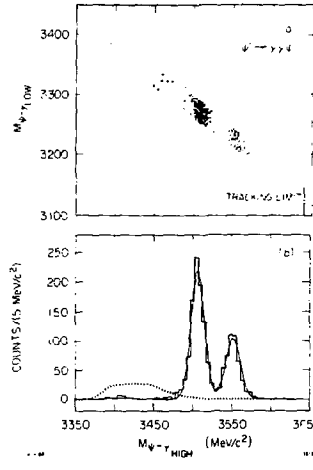

Fig. 4. Candidates for the cascade (2). (a) shows the scatterplot of higher and lower γ-ψ masses. (b) is its projection on the higher mass axis. The dotted curve is the Monte Carlo prediction for $\pi^0\pi^0$ background (magnified × 100).

ratios. The $\chi(3.41)$ mass is obtained from the ψ' inclusive γ spectrum; errors on the $\chi(3.51)$ and $\chi(3.55)$ include the 4 MeV/c^2 uncertainty in the mass of the ψ. In conclusion, we observe no evidence for an η_c' in the range 3129-3644 MeV/c^2 with a cascade branching ratio greater than 4×10^{-4}.

TABLE I

Mass (MeV/c^2)	$BR(\psi' \to \gamma'\chi) \cdot BR(\chi \to \gamma\psi)$
$3553.9 \pm 0.5 \pm 4$	$(1.26 \pm 0.09 \pm 0.20) \times 10^{-2}$
$3508.4 \pm 0.4 \pm 4$	$(2.38 \pm 0.12 \pm 0.38) \times 10^{-2}$
3413	$(0.059 \pm 0.015 \pm 0.009) \times 10^{-2}$
3.455 (0^{-+})	
e^+e^-, $\mu^+\mu^-$ final states:	$< 0.04 \times 10^{-2}$
only $\mu^+\mu^-$ final state :	$< 0.02 \times 10^{-2}$
3.591 (0^{-+})	$< 0.04 \times 10^{-2}$

VI. SPIN-MULTIPOLE STRUCTURE IN THE CASCADE

A study of the angular correlations among all particles in (2) furnishes information on multipole structure of the two photon transitions, as well as the χ spin (J_χ), however parity of the χ cannot be determined if the photon polarizations are not measured. The variables used in our cascade analysis are described in a paper by Karl, Meshkov and Rosner.[15] For clarity, I shall list the four stages of the cascade reaction:

$$e^+e^- \to \psi' \qquad (4a)$$

$$\psi' \to \gamma'\chi \qquad (4b)$$

$$\chi \to \gamma\psi \qquad (4c)$$

$$\psi \to \ell^+\ell^- \qquad (4d)$$

The cascade angular distribution $W(\cos\theta', \phi', \cos\theta_{\gamma\gamma}, \cos\theta, \phi; \underset{\sim}{p})$ is described by five measured angles, as well as parameters $\underset{\sim}{p}$ describing the multipole structure of the decays (4b) and (4c). The polar angles of γ' in the lab frame are denoted by θ' and ϕ', with the polar axis taken along the incident positron direction, and with $\hat{x}$ orthogonal to the two photon directions. Similarly, θ and ϕ describe γ in the ψ rest frame, with $\hat{z}$ along the direction of the final state positive lepton (or an average over ℓ^+ and ℓ^-); $\hat{x}$ is not altered by the boost to the ψ rest frame. The angle between the photons, in the χ rest frame, is $\theta_{\gamma\gamma}$.

Vectors used to obtain these angles are measured in different frames, accordant with the calculation for W; we may define them using the vectors $\hat{e}^+$ (the incident positron) and $\hat{\gamma}'$, both in the ψ' rest frame; $\hat{\gamma}$ in the χ rest frame; and $\hat{\ell}^+$ (the final positive lepton) in the ψ rest frame. All are unit vectors. Then,

$$\cos\theta' = \hat{e}^+ \cdot \hat{\gamma}' \qquad \tan\phi' = \frac{\hat{e}^+ \cdot (\hat{\gamma}' \times \hat{\gamma})}{\hat{e}^+ \cdot ((\hat{\gamma}' \times \hat{\gamma}) \times \hat{\gamma}')}$$

$$\cos\theta_{\gamma\gamma} = \hat{\gamma}' \cdot \hat{\gamma}$$

$$\cos\theta = \hat{\ell}^+ \cdot \hat{\gamma} \qquad \tan\phi = \frac{\hat{\ell}^+ \cdot (\hat{\gamma}' \times \hat{\gamma})}{\hat{\ell}^+ \cdot ((\hat{\gamma}' \times \hat{\gamma}) \times \hat{\gamma})}$$

The multipole parameters in W take the form

$$\Gamma(\chi \to \gamma\psi) \propto \sum_{j=1}^{J_\chi + 1} (a_1)^2$$

for (4c), and similarly for (4b). If the χ has even parity, then a_1 represents the E1 amplitude, a_2 the M2, and a_3 the E3 amplitude. The a_3 (octupole) amplitude is expected to be smaller than the a_2 (quadrupole) amplitude, which should in turn be smaller than the a_1 (dipole) amplitude. For this reason, we shall neglect a_3 in our analysis, bearing in mind that this approximation is valid only if a_2^2 is determined to be small. Then, after normalizing ($\Gamma \equiv 1$), we are left with only one multipole parameter for $J_\chi = 1$ or 2; the spin 0 case can only have a dipole amplitude. Denoting the quadrupole amplitude for (4c) by a_2, and the dipole amplitude by $\sqrt{(1-a_2^2)}$, the fitting variable is chosen to be $S(a_2)^2$, where S is the $\pm$ phase of a_2 relative to a_1. Similarly, S' and $(a_2')^2$ describe (4b).

Only $\chi(3.55)$ and $\chi(3.51)$ provide sufficient data for the angular correlation analysis. For each χ mass state, the fitting scheme consists of assuming a value for $J_\chi = 0,1$ or 2; then the data is compared to a Monte Carlo simulation using the parameters J_χ, $S'(a_2')^2$ and $S(a_2)^2$. A likelihhod function L is computed for each comparison involving an $(a_2')^2$-$(a_2)^2$ pair (which take the values $-1 \to 1$ in steps of 0.01). The function L is maximized over the $(a_2')^2$-$(a_2)^2$ grid to find the local maxima, and then absolutely maximized with a smooth fit. The largest of the three resulting $L(J_\chi)$ determines J_χ, a_2', and a_2 for each mass state.

The actual comparison of data with the Monte Carlo simulation is accomplished by binning the events over the 5 angles. To increase the statistics for each bin, we observe that W is symmetric under the angle transformations described by parity transformations. Parity conservation applies to each of the reactions in (4), hence we may parity transform combinations of (4a)-(4d)

so that 4 of the 5 angles are in the range 0-π; more precisely, we constrain $\cos\theta'$, $\cos\theta_{\gamma\gamma}$ and $\cos\theta$ to be positive, and ϕ' to have the range 0-π. Then, if the cosines are given bin sizes of 1/3, and ϕ' and φ bin sizes of π/3, the 5 angle histogram has a total of 486 bins. Such a binning allows for reasonable bin populations of the 921 χ(3.51) and 441 χ(3.55) data which have been fitted.

Our Monte Carlo simulator for each (J_x, a_2', a_2) parameter vector ($\underset{\sim}{p}$) incorporates the acceptances and efficiencies of the apparatus, as well as all the cuts applied to the real data; the real data is therefore binned directly, without correction for acceptance. Values for the likelihood function L are obtained by comparing the Monte Carlo produced and real data histograms. Since the sum of all histogram bins must equal the number of events observed, L is described by using a binomial probability density function[16]:

$$L(\underset{\sim}{p}) = N! \prod_{i=1}^{486} \frac{\langle n_i(\underset{\sim}{p})\rangle^{n_i}}{n_i!} \quad , \qquad N \equiv \sum_{i=1}^{486} n_i$$

where n_i is the number of data in bin i, and $n_i(\underset{\sim}{p})$ the Monte Carlo prediction for bin i.

The results of this analysis are summarized in Table II; the confidence level from χ^2 for each $L(\underset{\sim}{p})$ likelihood fit is shown.

TABLE II

Hypothesis	Confidence level	$S'(a_2')^2$	$S(a_2)^2$
χ(3.51) data:			
$J_x = 1$	0.15	+(0.7 ± 1.3)%	-(0.0 ± 0.4)%
$J_x = 2$	4×10^{-3}		
$J_x = 0$	$< 10^{-6}$		
χ(3.55) data:			
$J_x = 2$	0.22	+(2.7 ± 2.8)%	-(9.8 ± 10.0)%
$J_x = 1$	1×10^{-2}		
$J_x = 0$	3×10^{-4}		

Figure 5a,b shows the distribution of L in two particular instances, namely the maximum likelihood solutions over J_x. Each axis in Fig. 5 corresponds to one of the two photon transitions (4b) or (4c). The parameter $S(a_2)^2$ for each axis is written as "D", for a pure dipole ($a_1 = 1$, $a_2 = 0$) transition, "Q" for pure

quadrupole ($a_1 = 0$, $a_2 = 1$), "D+Q" for equal dipole and quadrupole amplitudes and a relative positive phase ($(a_2)^2 = \frac{1}{2}$, $S = +$), and "D-Q" for equal amplitudes with a relative negative phase ($S = -$). Both χ states have very nearly a D-D structure, as is expected in the charmonium model. Furthermore, the χ spin assignments are now quite firm: $\chi(3.51)$ has spin 1, hence $J^{PC} = 1^{++}$, and $\chi(3.55)$ clearly has $J^{PC} = 2^{++}$.

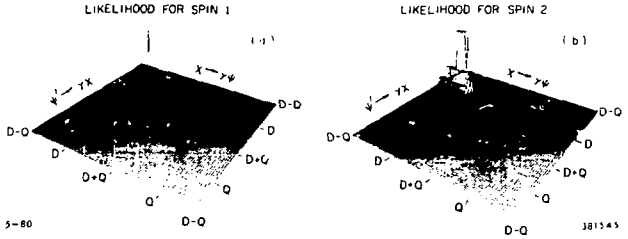

Fig. 5. Plots of the likelihood function $L(p)$ for fixed J_χ. (a) shows $L(J_\chi = 1)$ for the $\chi(3.51)$ data. (b) shows $L(J_\chi = 2)$ for the $\chi(3.55)$ data. The axes are explained in the text.

Spin information on the χ states can also be determined from the decay $\psi' \to \gamma'\chi, \chi \to \gamma\gamma$. The decay ${}^3P_{0,2} \to \pi^0\pi^0$ occurs in addition to the $\gamma\gamma$ mode, these pions having considerable energy. The photons from $\pi^0 \to \gamma\gamma$ thus have a small opening angle, and are reconstructed as a single photon with the tracking scheme described previously. For this reason, the initial candidates for $\psi' \to \gamma'\chi, \chi \to \gamma\gamma$ include events from $\chi \to \pi^0\pi^0$; the distribution of $(m_{\gamma\gamma})_{high}$ for these candidates is shown in Fig. 6a. The lower energy pion has a maximum laboratory momentum of 1.7 GeV/c, corresponding to a minimum opening angle of 9°. These angles are sufficiently large that the NaI(Tl) shower energy pattern of photons from the slower π^0 can be recognized as inconsistent with the expected pattern for a single photon, hence the $\pi^0\pi^0$ events can be subtracted from Fig. 6a, resulting in the distribution shown in Fig. 6b. These $\gamma\gamma$ and $\pi^0\pi^0$ distributions supply information on J^{PC} of the χ states, since ${}^3P_1$ cannot decay into $\gamma\gamma$ by Yang's theorem,[17] and cannot decay into $\pi^0\pi^0$ by parity conservation. From Figs 6a,b we conclude that: ${}^3P_{0,2} \to \pi^0\pi^0$, ${}^3P_1 \not\to \pi^0\pi^0$ or $\gamma\gamma$, ${}^3P_2 \to \gamma\gamma$, but there is no sign of ${}^3P_0 \to \gamma\gamma$. Preliminary branching ratios for $\chi \to \gamma\gamma$ are $(6 \pm 2) \times 10^{-4}$ for ${}^3P_2$, and an upper limit (90% C.L.) of 5×10^{-4} for ${}^3P_0$. These observed values are to be compared with the theoretical estimates[18] of 7×10^{-4} for ${}^3P_2$, and 13×10^{-4} for ${}^3P_0$.

VII. CONCLUSIONS

Now that the quantum numbers and cascade branching ratios for the $1^3P_{0,1,2}$ states are well established, it is possible to perform a test of the first order QCD theory for χ decay. Several authors[19] have pointed out that the most reliable calculation for $^3P_J \to$ gluons (or $^3P_J \to$ h, where "h" means hadrons) exists for the χ states with even spin, which may decay into 2 gluons in lowest order. The ratio $R = \Gamma(^3P_2 \to h)/\Gamma(^3P_0 \to h)$ has been calculated to be 0.27/0.02/0.40 for $J_P = 1^-/0^+/0^-$ gluons, respectively. To calculate R from the available measured quantities, we must assume that $\Gamma(^3P_J) = \Gamma(^3P_J \to \gamma\psi) + \Gamma(^3P_J \to h)$. Then, using $(7.1 \pm 2.0)\%$[20] for the initial branching ratio $BR(\psi' \to \gamma'\chi)$, we determine that $R = 0.12 \pm 0.03$. This result indicates a 5σ deviation from the vector gluon prediction, and corresponds to a measured rate for $^3P_0 \to \gamma\psi$ being one third of the QCD calculation.[21] The decays $^3P_{0,2} \to \gamma\gamma$ are analogous to the gluon processes. As in the $^3P_0 \to \gamma\psi$ case, $^3P_0 \to \gamma\gamma$ is observed with a rate less than one third of that expected. This discrepancy might be resolved when the radiative corrections are taken into consideration, however no calculation of these corrections has been made so far.

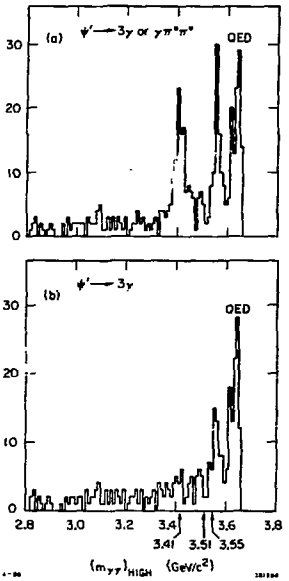

Fig. 6. Distribution of the higher $\gamma\gamma$ mass of candidates for $\psi' \to 3\gamma$. (a) shows the distribution before application of a pattern cut (described in the text) designed to eliminate π^0 which track as photons. (b) is the pattern-subtracted plot.

Results from multipole analysis are not so perverse. The E1 dominance for the transitions (4b,c) supports the use of the dipole approximation in the study of charmonium rates. The multipole result may also be applied to measure the magnetic moment of the charmed quark. In a recent paper, Karl, Meshkov and Rosner[22] have demonstrated the relation between a_2 (described previously) and the quark magnetic moment:

$$a_2 = \sqrt{(9/5)}\,(1+\kappa)\,\xi P_\gamma\,(4m_c)^{-1}\,, \quad (J_\chi = 2)$$

where ξ = + (−) for reaction 4b (4c), P_γ is the photon momentum, and m_c is the c-quark mass (we use 1.84 GeV/c^2). The magnetic moment is written as $(1+\kappa)\cdot\mu_{DIRAC}$, hence κ is the anomaly. Reactions (4b) and (4c) for the $^3P_1$ and $^3P_2$ data provide four measurements of κ. In all four cases, the phase of a_2 agrees with the observed multipole structure; the best measurement for κ comes from the $^3P_1$ data, from which we obtain a 90% C.L. limit $-2.1 < \kappa < +0.7$. Currently, we know of no detailed QCD calculation available to compare with our measured value.

ACKNOWLEDGEMENTS

It is a pleasure to thank J. Trân Than Vân for his assistance at Les Arcs, and for organizing this superb conference.

REFERENCES

1) R. Partridge, C. Peck, F. Porter (Caltech); D. Antreasyan, Y. F. Gu, W. Kollmann. M. Richardson, K. Strauch, K. Wacker (Harvard); D. Aschman, T. Burnett, M. Cavalli-Sforza, D. Coyne, H. Sadrozinski (Princeton); R. Hofstadter, R. Horisberger, I. Kirkbride, K. Königsmann, H. Kolanoski, A. Liberman, J. O'Reilly, J. Tompkins (Stanford); E. Bloom, F. Bulos, R. Chestnut, J. Gaiser, G. Godfrey, C. Kiesling, W. Lockman, M. Oreglia (SLAC).

2) E. D. Bloom, in Proc. of the 1979 Int. Symp. on Lepton and Photon Interactions at High Energies, ed. by T. Kirk and H. Abarbanel, p. 92 (also SLAC-PUB-2425) (1979).

3) C. Quigg, in Proc. of the 1979 Int. Symp. on Lepton and Photon Interactions at High Energies, ed. by T. Kirk and H. Abarbanel, p. 247 (1979).

4) J. S. Whitaker et al., Phys. Rev. Lett. 37, 1596 (1976).

5) W. Bartel et al., Phys. Lett. 79B, 492 (1978).

6) W. Tanenbaum et al., Phys. Rev. D17, 1731 (1978).

7) T. M. Himel, SLAC Report No. SLAC-223 (Ph.D. Thesis) (1979).

8) H. Frauenfelder and R. Steffen, in Alpha-, Beta-, and Gamma-Ray Spectroscopy, p. 997, ed. by K. Siegbahn, North-Holland, Amsterdam (1965).

9) E. D. Bloom, in Proc. of the XIVth Rencontre de Moriond, Les Arcs, France, ed. by J. Trân Than Vân (1979); Y. Chan et al., IEEE Trans. on Nucl. Sci., Vol. NS-25, No. 1, 333 (1978); I. Kirkbride et al., IEEE Trans. on Nucl. Sci., Vol. NS-26, No. 1, 1535 (1979).

10) A. Boyarski et al., Phys. Rev. Lett. 34, 1357 (1975); their value for BR($\psi \to e^+e^-$) is 0.069 ± 0.009.

11) T. M. Himel et al., Phys. Rev. Lett. 44, 920 (1980).

12) R. Brandelik et al., Nucl. Phys. B160, 426 (1979).

13) W. Tanenbaum et al., Phys. Rev. Lett. 36, 402 (1976).

14) G. Segre and J. Weyers, Phys. Lett. 62B, 91 (1976); N. Deshpande and E. Ma, Phys. Lett. 69B, 343 (1977); H. Genz, Lett. Nuovo Cimento 21, 270 (1978); R. Bhandari and L. Wolfenstein, Phys. Rev. D17, 1852 (1978); N. Isgur et al., Phys. Lett. 89B, 79 (1979); P. Langacker, Phys. Lett. 90B, 447 (1980); T. Pham, Ecole Polytechnique preprint PRINT 80-0330 (1980).

15) G. Karl, S. Meshkov and J. Rosner, Phys. Rev. D13, 1203 (1976).

16) W. Eadie *et al.*, Statistical Methods in Experimental Physics, North-Holland, Amsterdam (1971).

17) C. Yang, Phys. Rev. 77, 242 (1950).

18) T. Appelquist, R. Barnett and K. Lane, Ann. Rev. Nucl. Part. Sci. 28, 387 (1978).

19) M. Chanowitz and F. Gilman, Phys. Lett. 63B, 178 (1976); J. D. Jackson, Phys. Rev. Lett. 37, 1107 (1976).

20) C. Biddick *et al.*, Phys. Rev. Lett. 38, 1324 (1977).

21) J. D. Jackson, Phys. Lett. 87B, 106 (1979).

22) G. Karl, S. Meshkov and J. Rosner, PRINT-80-0225 (Minnesota) (1980).